MATHEMATICAL BIOSCIENCES
AND ENGINEERING
Volume **10**, Number **2**, April **2013**

doi:10.3934/mbe.2013.10.379

pp. **379–398**

AN EXTENSION OF GOMPERTZIAN GROWTH DYNAMICS: WEIBULL AND FRÉCHET MODELS

J. Leonel Rocha and Sandra M. Aleixo

Instituto Superior de Engenharia de Lisboa - ISEL, ADM and CEAUL
Rua Conselheiro Emídio Navarro, 1
1959-007 Lisboa, Portugal

(Communicated by Heiko Enderling)

Abstract. In this work a new probabilistic and dynamical approach to an extension of the Gompertz law is proposed. A generalized family of probability density functions, designated by $Beta^*(p,q)$, which is proportional to the right hand side of the Tsoularis-Wallace model, is studied. In particular, for $p=2$, the investigation is extended to the extreme value models of Weibull and Fréchet type. These models, described by differential equations, are proportional to the hyper-Gompertz growth model. It is proved that the $Beta^*(2,q)$ densities are a power of betas mixture, and that its dynamics are determined by a non-linear coupling of probabilities. The dynamical analysis is performed using techniques of symbolic dynamics and the system complexity is measured using topological entropy. Generally, the natural history of a malignant tumour is reflected through bifurcation diagrams, in which are identified regions of regression, stability, bifurcation, chaos and terminus.

1. **Introduction.** In recent decades, the growth models, whether populational or tumoral, has been one of the research topics of greatest relevance. The number of phenomenological growth models based on competition of two terms, one representing the production and the other associated with death, is amazingly large. Consider all particular cases of the generalized logistic model and also of the Tsoularis-Wallace-Schaefer model, among other models studied, see [13], [14], [24], [27] and references therein.

The Gompertzian model of growth was initially introduced as an actuarial function for the study of aging processes. Nowadays, the Gompertz function is widely used with success in demographic, economic, ecological, biological and medical studies. Its application is highlighted in gene expression, enzyme kinetics, oxygenation of hemoglobin, intensity of photosynthesis and in the growth of organisms, cells, organs, tissues, tumours or populations, among other topics of investigation, see for example [7], [8], [9], [25], [29] and [32].

The Gompertz function plays an important role in the extreme value theory, where it is known as Gumbel distribution function. The Gumbel extreme stable

2010 *Mathematics Subject Classification.* Primary: 92D25, 91B62, 62H10, 11S82; Secondary: 92B05, 37H20, 37B10, 37B40.

Key words and phrases. Growth models, extreme value laws, $Beta^*(p,q)$ densities, bifurcations and chaos, symbolic dynamics, topological entropy, tumour dynamics.

The authors are supported by National Funds through FCT — Fundação para a Ciência e a Tecnologia, project PEst-OE/MAT/UI0006/2011, and PTDC/FEDER.

law has in its domain of attraction laws with infinite right endpoint and others with finite right endpoint, [20]. In fact, laws in the Gumbel model domain of attraction are not heavy tailed, and this can be a serious drawback for the Gompertz growth model studied by Laird and Waliszewski, among others, as a cancer growth model, see for example [8], [9] and [32]. An extension of the differential equation, whose solution is the Gompertz function, leads to the Fréchet or Weibull extremes value models, which for appropriate values of the shape parameter can be very heavy or light tailed, respectively.

As in the Gompertz model, our models predict infinite growth rates for small tumors. Hence, the tumour free equilibrium is unstable. So, it is verified that the immune system would never be able to totally suppress even the smallest tumour cell aggregates, which is a strong inference. The medical implications that come from there are deep, i.e., the impossibility to completely recover from any type of tumors whatsoever. On the contrary, it is usual to assume that the immune system may be able, in some cases, to kill a relatively small aggregate of cancer cells. Underlying cancer therapies is implicit the assumption that the drug will kill the vast majority of malignant cells, and the remaining residual cells may, in certain cases, be eliminated by the immune system. Given this hypothesis, the tumour free equilibrium should have the possibility to be locally asymptotically stable, and as a consequence, the growth rates for small tumours should be bounded. This discussion has been the subject of several studies, see for example [18] and references therein. In future work, we intend to address this limitation in our models.

One of the greatest contributions of this work is the study and discussion of new growth models, defined by ordinary differential equations, whose particular solutions are extreme value distributions of Weibull and Fréchet type. Some authors have observed that the major limitation of Verhulst and Gompertz models was the inflexibility of the inflection point, which leads to consider the number of individuals or cells, when the growth rate is maximum, always constant, see for example [27]. The models of Weibull and Fréchet type under investigation have the great advantage of consider that the number of individuals or cells, when the growth rate is maximum, can be variable. The inflection points associated to these models converge to a fix number in the Gompertz model. We remark that, these models lead to a wide diversity of dynamics and its retardation factors are of polynomial type. The dynamical study of these growth laws depends on two parameters: the intrinsic growth rate of the number of individuals or cells and the growth-retardation factor.

In previous studies, Aleixo *et al* [1], [2] and [3], presented a new dynamical approach to study population growth models, proportional to $Beta(p, 2)$ densities, based on natural extensions of the logistic Verhuslt model. In the present work, we investigate a family of probability density functions tied to the classical beta family, designated by $Beta^*(p, q)$. These density functions are proportional to the right hand side of the growth models under study. Some of these densities are generalized Pareto, that span the possible regular variation of tails. More specifically, we extend the investigation to other extreme stable models, namely Weibull's and Fréchet's types in the General Extreme Value (GEV) model.

The layout of this paper is as follows. In Sec.2, we present some preliminaries notions and results on $Beta^*(p, q)$ probability density functions and Gompertz growth models. Sec.3 is devoted to the study and investigation of Weibull and

Fréchet growth type models, defined as ordinary differential equations. In a probabilistic approach, made in Sec.4, we prove that these models are powers of a mixture of betas densities. Our more versatile family of models inherits and amplifies the interplay between Malthusian growth term and retroactive term of the logistic parabola, which results in an interesting heavy and light tail equilibrium result. The difference equations correspondent to the Weibull and Fréchet growth models are interpreted as non-linear coupling of probabilities, which determine Frechetzian and Weibullzian dynamics. Then, in Sec.5, we consider dynamical systems defined as a family of unimodal maps proportional to $Beta^*(2,q)$ densities, with $q>1$. The complex dynamical behaviour of these maps is developed and investigated using iteration theory and symbolic dynamics. This dynamical analysis is characterized on a parameter space, which is split into different regions, according to the chaotic behaviour of the models, in terms of topological entropy. This characterization reflects the natural history of the malignant tumour. At last, we discuss our numerical results and provide some relevant conclusions.

2. **Preliminaries.** In this section, we introduce some notions and basic results on probability density functions and the correspondent growth models. A particular attention is given to the Gompertz growth model.

Observing that the logistic parabola

$$f_{r,2,2}(x) = \ r\ x\ (1-x) \tag{1}$$

is proportional to the $Beta(2,2)$ density, where $x\ \in\ [0,1]$ and $r>0$ is the Malthusian parameter, Aleixo *et al*, [1], [2] and [3], investigated the complex dynamical behaviour of some models of the type

$$f_{r,p,q}(x) = \ r\ x^{p-1}\ (1-x)^{q-1}$$

which are proportional to $Beta(p,q)$ densities[1], with $x\ \in\ [0,1]$ and $p,q>1$ shape parameters. The dynamics of these probabilistic models were studied in the parameter space, in terms of topological entropy. In particular case of $q=2$, these models are typically used to study populations of whales and forest fires. The parameter p measures the difficulty of the mating process. In forest fire models it expresses the number of burning trees necessary to set fire to a green tree, [5]. Note that, the equation introduced by Blumberg, [4], which is called as hyperlogistic law, its right hand side is proportional to $Beta(p,q)$ densities. The dynamical analysis of the growth models related to Blumberg's equation is presented in [23].

In Pestana *et al*, [21], is considered an extension of the beta function and of the beta densities to develop a general approach of Verhulst growth model, leading to the Gompertz function. Observe that,

$$-\ln x = \sum_{k=1}^{\infty} \frac{(1-x)^k}{k} \tag{2}$$

when $x\to 0$, so the Euler's Beta function

$$B(p,q) = \int_0^1 \ x^{p-1}\ (1-x)^{q-1}\ dx$$

[1]If X is a random variable with $Beta(p,q)$ distribution, denoted by $X\frown Beta(p,q)$, then the corresponding probability density function is $h_{p,q}(x) = \ \frac{1}{B(p,q)}\ x^{p-1}\ (1-x)^{q-1} I_{(0,1)}, p,q>0$, where $B(p,q)$ is the Euler's beta function.

may be viewed as a first order approximation of a non-trivial extension of

$$B^*(p,q) = \int_0^1 x^{p-1} \, (-\ln x)^{q-1} \, dx.$$

The main purpose of this work is to study a new family of probability density functions, which for certain values of the parameters includes the Gompertz model and models of Weibull and Fréchet type. This claim is attained using the first order approximation of the function $-\ln x$ on the $Beta(p,q)$ probability density function $h_{p,q}(x)$, as introduced in [21]. A new probabilistic model designated by $Beta^*(p,q)$, whose probability density function, denoted by $h^*_{p,q}(x)$, is defined by

$$h^*_{p,q}(x) = \frac{1}{B^*(p,q)} \, x^{p-1} \, (-\ln x)^{q-1} \, I_{(0,1)} \tag{3}$$

with $p,q>0$, $\frac{1}{B^*(p,q)} = \frac{p^q}{\Gamma(q)}$, where $\Gamma(q) = \int_0^{+\infty} x^{q-1}e^{-x}dx$ is the gamma function. Remark that, the function $B^*(p,q)$, defined above, plays a similar role to the of Euler's Beta function in the probability density function of the usual Beta distribution.

Note that, the right hand side of the Tsoularis-Wallace model, defined in [27], is proportional to the $Beta^*(p,q)$ densities. It is also to emphasize that, the right hand side of the hyper-Gompertz law proposed by Turner *et al* in [28], as a limit case of a general class of three-parameters power-law models, which includes the so called hyper-logistic law, is proportional to the $Beta^*(2,q)$ densities. Also, the right hand side of the generalized Gompertz model, suggested by Marušić *et al* in [14], is proportional to the $Beta^*(p,2)$ densities. In [13] and [19], readers can find many more details, approaches and references.

In particular, the probabilistic model described by $Beta^*(2,2)$ density

$$h^*_{2,2}(x) = 4 \; x \; (-\ln x) \; I_{(0,1)} \tag{4}$$

is proportional to the normalized Gompertz derivative

$$\frac{df_N(t)}{dt} = \; b \; f_N(t) \; \left(-\ln f_N(t)\right), \; \text{with} \;\; b>0. \tag{5}$$

The interest of the $Beta^*(2,2)$ model lies in the construction of an extension of the Verhulst model. This show that, stable laws for maxima provide a natural framework to study growth when some external behavior is expected, as in the case of cancer growth. A particular solution of the differential equation (5) is the normalized Gompertz function given by

$$f_N(t) = e^{-e^{-bt}} \tag{6}$$

which represents a normalized number of individuals or cells at time t (t is a dimensionless variable given in some specific units). This function defines the Gompertzian distribution, for $t \in \mathbb{R}$, which has a sigmoid curve representation, see Fig.1. From an initial population size $f_N(t_0)$, at an initial time t_0, growth models are used to predict the size $f_N(t)$ of the population at an arbitrary time $t > t_0$.

The interpretation of the graphic of Eq.(6) was made by Laird, in order to compare dynamics of tumour growth in several host organisms. In this context, the growth data for all analyzed malignant tumours have been overlapped after adjustment of the units on the two axes, with the inflection point of the Gompertz curve

as the point of reference, [9]. Note that, the number of cells at the inflexion point of the Gompertz sigmoid curve

$$f_N(0) = e^{-1} = N_{inf}$$

corresponds to the number of cells when the growth rate is maximum. So, the inflexion point for the Eq.(6) is fixed for any parameter $b > 0$, see Fig.1.

The differential equation (5) suggests that at least two different dynamic processes states dynamics of tumour growth. The analysis of this equation confirms that the coupling of the probabilities has a complex and non-linear algebraic form, see Sec.4.

In general, the differential equation

$$\frac{df(t)}{dt} = a\ b\ e^{-bt}\ f(t) \tag{7}$$

usually designated by derivative of the Gompertz function, admits as a solution the sigmoid Gompertz function, given by

$$f(t) = e^{a\left(1-e^{-bt}\right)}$$

in which $f(t)$ is the number of tumour cells or their weight at time t, a and b are experimental coefficients determining the slope of the curve. These coefficients can also be interpreted as $a = \frac{\gamma_0}{\beta}$ and $b = \beta$, where γ_0 is the initial growth rate in biological scale or proliferation rate and β is the retardation factor, [17]. This function can represent the growth curve for neuron-like differentiating cells or malignant tumours, [29]. The derivative of the Gompertz function, given by Eq.(7), reflects the speed of tumour growth. As a particular case, when the retardation factor tends to zero, the Gompertz function is the exponential growth model, [8], [29] and [30].

Note that, considering the normalized Gompertz solution of Eq.(5)

$$f_N(t) = f_N(t_0)\ e^{-e^{-bt}} \ \Leftrightarrow\ e^{-bt} = -\ln\frac{f_N(t)}{f_N(t_0)}$$

replacing in Eq.(7) we obtain the normalized Gompertz differential equation

$$\frac{df_N(t)}{dt} = a\ b\ f_N(t)\ \left(-\ln\frac{f_N(t)}{f_N(t_0)}\right) \tag{8}$$

which will allow to deduce the corresponding difference equation in Sec.4.

3. **Gompertz growth model and extensions.** The logistic parabola Eq.(1) can be transformed to the algebraic form of a differential equation, if the time t is a continuous entity, given by

$$\frac{df_N(t)}{dt} = b\ f_N(t)\ \left(1 - f_N(t)\right).$$

This equation produces a symmetric bell-shaped curve. Several works were developed in order to study more complex models which exhibit asymmetry, namely introducing power exponents in the logistic equation, see for example [1] and [3], obtaining

$$\frac{df_N(t)}{dt} = r\ f_N(t)^{p-1}\ \left(1 - f_N(t)\right)^{q-1},\ \text{with}\ \ p, q > 1$$

where r is the Malthusian parameter, p and q are shape parameters. Note that, we consider the shape parameters $p, q > 1$, because for $0 < p, q \leq 1$ the models under study cannot be studied as unimodal maps, see Sec.5. Taking into account the series expansion given by Eq.(2), the differential equation (5), which represents the

normalized Gompertz derivative, is generalized by introducing power exponents, as follows

$$\frac{df_N(t)}{dt} = b\, f_N(t)^{p-1}\ (-\ln f_N(t))^{q-1}, \text{ with } p,q>1 \tag{9}$$

leading to more complex models, with another kind of skewness. The parameter b is proportional to the retardation factor and is an experimental coefficient that determines the slope of the curve. We remark that, the normalized number of individuals or cells at time t, $f_N(t)$, given by Eq.(6), verifies $0 < f_N(t) \leq 1$, hence the Eq.(9) does not include complex numbers.

In particular, if $p = q = 2$ in Eq.(9) then the normalized Gompertz derivative Eq.(5) is obtained. Considering the parameters $p = 2$ and $1 < q < 2$, the differential equation (9) models growths governed by Weibull distribution. On the other hand, if $p = 2$ and $q > 2$ then the differential equation (9) leads to Frechetzian growths. In the next subsections, growth models governed by Weibull and Fréchet distributions are studied.

3.1. **Models of Weibull type.** The expression of the normalized differential equation, that defines growth models of Weibull type, is given by

$$\frac{df_N(t)}{dt} = c\, f_N(t)\ (-\ln f_N(t))^{1-\frac{1}{\alpha}}, \text{ with } 0 < \frac{1}{\alpha} < 1. \tag{10}$$

This model has light left tail and finite right endpoint, see Fig.3(a). Attending to an adequate variable change, this ordinary differential equation has a particular real solution, for $c = 1$,

$$f_N(t) = e^{-(-t)^{\alpha}}, \text{ with } t \in \mathbb{R}.$$

Considering a restriction of this particular solution for $t \in]-\infty, 0[$ and stating that $f_N(t) = 1$, for $t \geq 0$, becomes defined a Weibull$-\alpha$ extreme value distribution, [20], i.e.,

$$f_N(t) = \begin{cases} e^{-(-t)^{\alpha}} & \text{if } t < 0 \\ 1 & \text{if } t \geq 0 \end{cases}. \tag{11}$$

The graphics of this family of functions, which we designated by normalized Weibull functions, are sigmoidal curves, with $0 < f_N(t) \leq 1$, see Fig.1. In this work, the generalization parameter α is related to the growth-retardation phenomena. Of course the physical meaning of parameters has to be adapted to the one assumed by $f_N(t)$. The difference equation counterpart generates Weibullzian dynamics, see Subsec.4.2.

Note that, the number of cells at the inflexion point of the Weibull sigmoid curve

$$f_N\left(-\left(\frac{\alpha-1}{\alpha}\right)^{\frac{1}{\alpha}}\right) = e^{-\left(1-\frac{1}{\alpha}\right)} = N_{inf} \tag{12}$$

that corresponds to the number of cells when the growth rate is maximum, satisfies

$$0 < N_0 < e^{-1} < N_{inf} < 1 \tag{13}$$

where $N_0 = f_N(t_0)$ is the number of cells at the initial time t_0. Indeed, the second inequality is necessary to achieve the number of cells at the inflexion point. If $\frac{1}{\alpha} \to 0$ then $N_{inf} \to e^{-1}$, i.e., for large values of α is attained the number of cells when the growth rate is maximum for the Gompertz function. On the other hand, if $\frac{1}{\alpha} \to 1$ then $N_{inf} \to 1$, i.e., when $\alpha \to 1$ the number of cells when the growth rate is maximum tends to the normalized carrying capacity, see Fig.1.

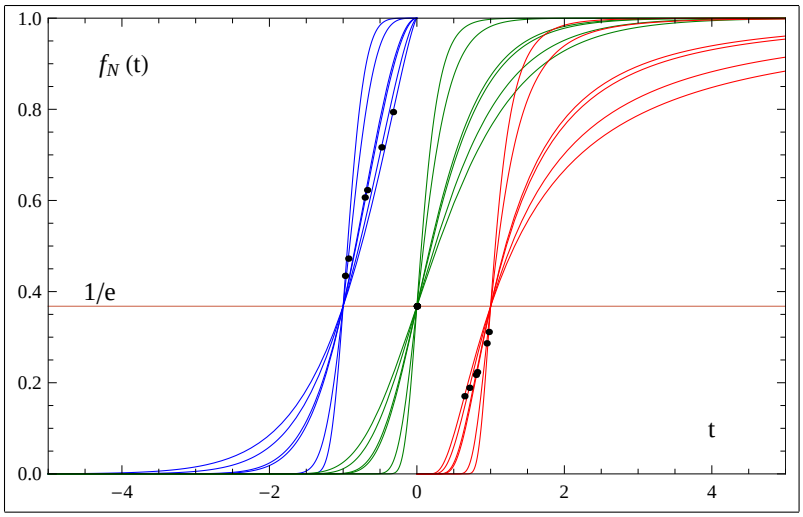

FIGURE 1. Normalized sigmoidal curves: Weibull (left), Gompertz (center) and Fréchet (right), with $\alpha = b = 1.3, 1.5, 1.9, 2, 4, 6$. At the center, we have the sigmoid representation of the Eq.(6), the normalized Gompertz curves, where the inflexion point is fixed for any parameter b. At the left, the sigmoid normalized Weibull curves of the Eq.(11) are presented, where the number of cells at the inflexion point verify $N_{inf} \to e^{-1}$, when $\frac{1}{\alpha} \to 0$, see Eqs.(12) and (13). At the right, we have the normalized Fréchet curves of the Eq.(19), where the number of cells at the inflexion point verify $N_{inf} \to e^{-1}$, when $\frac{1}{\alpha} \to 0$, see Eqs.(20) and (21).

The normalized Weibull function Eq.(11) satisfies the Banach fixed point theorem (in Banach space of real numbers), because the normalized Weibull derivative is a contraction mapping, i.e.,

$$f'_N(t) = \alpha(-t)^{\alpha-1}\, e^{-(-t)^\alpha} \leq f_N(t) \leq 1 \tag{14}$$

with $\alpha > 1$ and $t \to +\infty$. This property confers a fractal structure to the curve generated by Eq.(11).

In a general way, the Weibull function is defined by the expression

$$f(t) = e^{a(1-(-t)^\alpha)} \tag{15}$$

which is a particular solution of the differential equation

$$\frac{df(t)}{dt} = a\ \alpha(-t)^{\alpha-1} f(t). \tag{16}$$

Note that, considering the normalized Weibull solution

$$f_N(t) = f_N(t_0)\ e^{-(-t)^\alpha} \Leftrightarrow (-t)^{\alpha-1} = \left(-\ln \frac{f_N(t)}{f_N(t_0)}\right)^{\frac{\alpha-1}{\alpha}}$$

and replacing in the differential equation (16), we obtain

$$\frac{df_N(t)}{dt} = a\ \alpha\ f_N(t) \left(-\ln \frac{f_N(t)}{f_N(t_0)}\right)^{1-\frac{1}{\alpha}}. \tag{17}$$

3.2. **Models of Fréchet type.** In this work are also studied growth models of Fréchet type, which are defined by the normalized differential equation

$$\frac{df_N(t)}{dt} = c\ f_N(t)\ \left(-\ln f_N(t)\right)^{1+\frac{1}{\alpha}},\ \text{with}\ \frac{1}{\alpha} > 0. \tag{18}$$

Laws in the extreme value Fréchet domain of attraction for maxima must have infinite right endpoint, and can be severely heavy-tailed. Its right tail is heavier than in the standard gaussian, which is in the Gumbel domain of attraction, see Fig.3(c). The difference equation associated to Eq.(18) generates the Frechetzian dynamics, see Subsec.4.2. A particular real solution of Eq.(18), for $c = 1$, takes the form

$$f_N(t) = e^{-t^{-\alpha}},\ \text{with}\ \ t \in \mathbb{R}.$$

Considering now a restriction of this particular solution for $t \in]0, +\infty[$, and claiming that $f_N(t) = 0$, for $t \leq 0$, it results in the Fréchet$-\alpha$ extreme value distribution, [20], i.e.,

$$f_N(t) = \begin{cases} 0 & \text{if } t \leq 0 \\ e^{-t^{-\alpha}} & \text{if } t > 0 \end{cases} \tag{19}$$

which we designated by normalized Fréchet function, with $0 < f_N(t) \leq 1$, see Fig.1.

In this case, the number of cells at the inflexion point of the Fréchet sigmoid curve

$$f_N\left(-\left(-\frac{\alpha}{1+\alpha}\right)^{\frac{1}{\alpha}}\right) = e^{-\left(1+\frac{1}{\alpha}\right)} = N_{inf} \tag{20}$$

satisfies

$$0 < N_0 < N_{inf} < e^{-1}. \tag{21}$$

If $N_{inf} < N_0$ then the inflexion point is near the origin and the number of cells must be considered at the initial time N_0, ensuring that the N_{inf} is never attainable, [27]. This extreme behavior is reflected in the existence of the spontaneous extinction or the regression tumour region, that ensure the possibility of immune surveillance, see Subsec.5.1. When $\frac{1}{\alpha} \to 0$, the upper bound of the normalized number of cells growth corresponds to the number of cells when the growth rate is maximum for the Gompertz function, see Fig.1.

The Banach fixed point theorem is satisfied by the normalized Fréchet function (19), as follows

$$f'_N(t) = \alpha t^{-(\alpha+1)} e^{-t^{-\alpha}} \leq f_N(t) \leq 1 \tag{22}$$

with $\alpha > 0$ and $t \to +\infty$. The mapping with these features, given by Eq.(19), generates a fractal curve. Note that, the derivative reflects the speed of the tumour growth.

In general, the differential equation of the first order

$$\frac{df(t)}{dt} = a\ \alpha\ t^{-(\alpha+1)}\ f(t) \tag{23}$$

has the particular solution

$$f(t) = e^{a\left(1-t^{-\alpha}\right)} \tag{24}$$

which is designated by Fréchet function. Note that, the parameter α in Eqs.(15) and (24) plays the role of the retardation factor. While in the Gompertz model, proposed by Laird in [8] and [9], the retardation factor is of exponential type, in the Weibull and Fréchet models, investigated in this work, this retardation factor is of polynomial type.

Attending to that, the normalized Fréchet solution

$$f_N(t) = f_N(t_0)\ e^{-t^{-\alpha}} \Leftrightarrow\ t^{-(\alpha+1)} = \left(-\ln \frac{f_N(t)}{f_N(t_0)}\right)^{\frac{\alpha+1}{\alpha}}$$

and, replacing in Eq.(23), we obtain the normalized Fréchet differential equation

$$\frac{df_N(t)}{dt} = a\ \alpha f_N(t)\ \left(-\ln \frac{f_N(t)}{f_N(t_0)}\right)^{1+\frac{1}{\alpha}}. \tag{25}$$

The feature of the Eqs.(16) and (23) suggests that at least two different dynamic processes determine dynamics of the Weibullzian and Frechetzian growths, where one of the processes is determined by an approximation of the exponential function. Observing Fig.1, it can be evidenced that the sigmoid Weibullzian and Frechetzian curves generated by Eqs.(11) and (19), respectively, can be divided into three segments, as Laird defined for the Gompertz function. The first segment is defined until the inflexion point. In this part, the curve is concave upwards, and represents the dynamics of the initial stages of tumour development. The second one, is defined from the inflexion point until the later time point, where the growth rate stabilizes, and reflects dynamics of tumour growth until the death of the tumour-host system. The last segment describe the dynamics of the system if the host has continued to live, [8], [9] and [29].

Remark. It is important to emphasize that, the length of these segments are different according to the type of the model and to the respective parameters values, stating that the dynamics of tumour progression is different in each interval of the natural history of malignant tumour, see Fig.1:

- The Weibull type models describe tumour growths in which the initial growth phase is very long. After the initial growth phase, the period of time of the tumor development until dead is very short.
- The Fréchet type models represent tumour growths in which the initial growth phase is short. The period of the tumour development to the death is highly variable, i.e., the tumor growth can stabilize near reaching the carrying capacity or can take a long time to reach this value.

Generally, as bigger the value of the parameter α, smaller is the time for the sigmoid growth curve to reach the carrying capacity. Therefore, the models proposed could be considered as having the basic ingredients to model more complex and irregular types of growths of tumourigenesis of several human and animal malignancies. In Subsec.5.1 is presented a more detailed and complex approach of the tumour growth, using the theory of dynamical systems.

4. **Probabilistic approach.** In a previous work [21] it was shown that the $Beta^*(2,2)$ probability density function $h^*_{2,2}(x)$, given by Eq.(4), is a convex mixture of the $Beta(2,k+1)$ densities, with weights w_k, i.e.,

$$h^*_{2,2}(x) = \sum_{k=1}^{\infty} w_k\ h_{2,k+1}(x) = \sum_{k=1}^{\infty} \frac{4}{k\,(k+1)\,(k+2)}\ h_{2,k+1}(x)$$

where $\sum_{k=1}^{\infty} w_k = 1$. On the other hand, it was proved that each $h_{2,k+1}(x)$ is a signed mixture of $Beta(j+2,1)$ densities with weights w_j^*, i.e.,

$$h_{2,k+1}(x) = \sum_{j=0}^{k} w_j^* \; h_{j+2,1}(x) = \sum_{j=0}^{k} \frac{(-1)^j \; \binom{k}{j}}{B\,(2,k+1)\,(j+2)} \; h_{j+2,1}(x)$$

where $\sum_{j=0}^{k} w_j^* = 1$. Therefore, the $Beta^*(2,2)$ probability density function $h_{2,2}^*(x)$ is a signed mixture of $Beta(j+2,1)$ densities, with weights

$$w_{kj}^{**} = \frac{4\;(-1)^j \; \binom{k}{j}}{k\,(j+2)}, \quad \text{where} \sum_{k=1}^{\infty}\sum_{j=0}^{k} w_{kj}^{**} = 1.$$

So, the $Beta^*(2,2)$ probability density function, proportional to Gompertz growth model, is a signed mixture of power laws with natural exponents. In this growth law, each positive even component that contributes to the growth rate is moderated by the retroaction of the next negative odd term.

Furthermore, in several works it was suggested that at least two different dynamics processes determine dynamics of tumour growth, [8], [29] and [30]. In particular, from Eq.(8) and attending to Euler's algorithm, it is usual to consider the model of growth (when there is a limit to growth) given by the difference equation

$$p_{n+1} = r \; p_n \,(-\ln p_n) + p_n \tag{26}$$

where $r = a \; b \; \Delta_t$, with $\Delta_t \to 0$, $p_n = \frac{f_N(t_n)}{f_N(t_0)}$, with initial value p_0, and time t is measured in time-steps, $n \in \mathbb{N}$. This equation is also known as the iterative normalized Gompertz function. In fact, the Gompertzian distribution represents a coupling of probabilities, [29], [31] and [30]. We note that, as stated by Waliszewski and Konarski in [30], the Eq.(26) generates a Feigenbaum-like diagram, see Fig.2(b). However, to be observed a chaotic behavior in this model is necessary to consider $2.5357 < r < 2.7184$, see numerical results of Table 1.

The number of cells in the $(n+1)^{th}$ generation is represented by p_{n+1} and p_n is a number (fraction or probability) of cells undergoing divisions in the n^{th} generation. The expression $1-p_n$ is interpreted as a first order linear discrete approximation of $-\ln p_n$, meaning the approximate number (fraction or probability) of cells among the population of the n^{th} generation which do not divide. Thus, Eq.(26) has a similar algebraic structure to the logistic difference equation. In the n^{th} step iteration, this difference equation describe the co-existence of two antagonistic processes or events, one with probability p_n and the other with "approximate" probability $1-p_n$.

In next subsections, we extend the above probabilistic approaches to the Weibull and Fréchet growth models type.

4.1. $Beta^*(2,q)$ **models as a power of betas mixture.** In this context, it is proved that the $Beta^*(2,q)$ probability density function, with $q > 1$, proportional to the hyper-logistic growth law, is a power of mixture of beta densities. Considering

Eqs.(3) and (2), we can write

$$h^*_{2,q}(x) = \frac{1}{B^*(2,q)}\; x\; (-\ln x)^{q-1} = \frac{2^q}{\Gamma(q)}\; x \left(\sum_{k=1}^{\infty} \frac{(1-x)^k}{k}\right)^{q-1}$$
$$= \left(\sum_{k=1}^{\infty} \left(\frac{2^q}{\Gamma(q)}\right)^{\frac{1}{q-1}} \frac{1}{k}\; x^{\frac{1}{q-1}}\; (1-x)^k\right)^{q-1} = \left(\sum_{k=1}^{\infty} \widetilde{w}_k\; h_{\frac{q}{q-1},k+1}(x)\right)^{q-1}$$

with weights

$$\widetilde{w}_k = \left(\frac{2^q}{\Gamma(q)}\right)^{\frac{1}{q-1}} \frac{B\left(\frac{q}{q-1}, k+1\right)}{k}, \quad \text{where } \sum_{k=1}^{\infty} \widetilde{w}_k = 1.$$

Thus, the $Beta^*(2,q)$ densities $h^*_{2,q}(x)$ are described as powers of order $q-1$ of mixture of $Beta\left(\frac{q}{q-1}, k+1\right)$ densities $h_{\frac{q}{q-1},k+1}(x)$, with $q > 1$ and $k \in \mathbb{N}$. On other hand, these $Beta\left(\frac{q}{q-1}, k+1\right)$ densities can be rewritten as follows,

$$h_{\frac{q}{q-1},k+1}(x) = \frac{1}{B(\frac{q}{q-1}, k+1)}\; x^{\frac{1}{q-1}}\; (1-x)^k = \sum_{j=0}^{k} \widetilde{w}^*_j\; h_{j+\frac{q}{q-1},1}(x)$$

with weights

$$\widetilde{w}^*_j = \frac{(-1)^j\; \binom{k}{j}\, B\left(j+\frac{q}{q-1}, 1\right)}{B\left(\frac{q}{q-1}, k+1\right)}, \quad \text{where } \sum_{j=0}^{k} \widetilde{w}^*_j = 1.$$

Therefore, the Weibull and Fréchet growth models type are powers of order $q-1$ of mixture of $Beta\left(j+\frac{q}{q-1}, 1\right)$ densities $h_{j+\frac{q}{q-1},1}(x)$, i.e.,

$$h^*_{2,q}(x) = \left(\sum_{k=1}^{\infty}\sum_{j=0}^{k} \frac{(-1)^j\; \binom{k}{j}}{k}\; \left(\frac{2^q}{\Gamma(q)}\right)^{\frac{1}{q-1}} B\left(j+\frac{q}{q-1}, 1\right)\; h_{j+\frac{q}{q-1},1}(x)\right)^{q-1}.$$

The above results allow us to conclude that, in the models under study each positive even component, that propels the growth, is moderated by the retroaction of the next negative odd term. These power laws include regularly varying tailed models but also asymptotic extreme value models. These phenomena occur in malignant tumor cell populations.

4.2. **Non-linear coupling of probabilities determines Weibullzian and Frechetzian dynamics.** In a first approach, simple coupling of probabilities for two dynamic processes opposite to each other is not sufficient to generate Gompertzian dynamics. It is necessary to consider a non-linear coupling of these antagonistic processes. The typical asymmetric plot of the Gompertz derivative (7) emerges if more complex coupling takes place. The models of Weibull and Fréchet type described above, given by the Eqs.(10) and (18), respectively, exhibit behaviors whose asymmetry is more pronounced, see Figs.1 and 3.

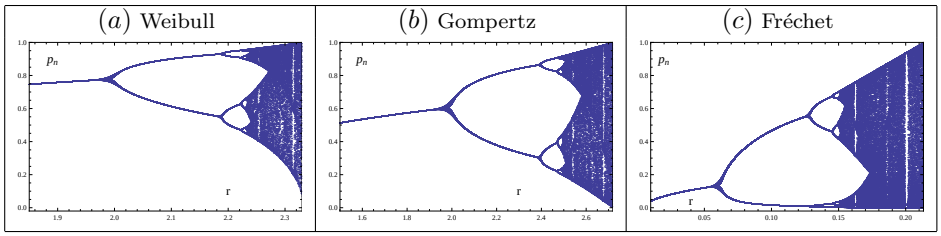

FIGURE 2. Bifurcation diagrams generated by the normalized iterative equations: Weibullzian dynamics (Eqs.(17) and (27), with $\alpha = 2$), Gompertzian dynamics (Eqs.(8) and (26)) and Frechetzian dynamics (Eqs.(25) and (28), with $\alpha = \frac{1}{3}$). Consecutive bifurcations lead that systems towards deterministic chaos. In the models of Gompertz and Weibull types, chaotic behavior is only observable for high values of r. Furthermore, in the models of Fréchet type it is possible to identify chaotic behavior for small values of r, see Fig.4.

The discretization of the Eq.(17) is obtained, applying Euler's algorithm, as follows

$$\begin{aligned}
&\frac{f_N(t_{n+1}) - f_N(t_n)}{\Delta_t} = a\alpha f_N(t_n)\left(-\ln\frac{f_N(t_n)}{f_N(t_0)}\right)^{1-\frac{1}{\alpha}}\\
&\Leftrightarrow f_N(t_{n+1}) = r\ f_N(t_n)\left(-\ln\frac{f_N(t_n)}{f_N(t_0)}\right)^{1-\frac{1}{\alpha}} + f_N(t_n)\\
&\Leftrightarrow p_{n+1} = r\ p_n\left(\frac{1}{r} + (-\ln p_n)^{1-\frac{1}{\alpha}}\right)
\end{aligned} \tag{27}$$

with $r = a\ \alpha\ \Delta_t$, $\Delta_t \to 0$, $p_n = \frac{f_N(t_n)}{f_N(t_0)}$ and $0 < \frac{1}{\alpha} < 1$. This difference equation is designated by iterative normalized Weibull equation. The quantities involved in this equation are analogous to the Eq.(26). The Eq.(27) describes a non-linear coupling of probabilities, between two "quasi" antagonistic processes, that determine the Weibullzian dynamics. The algebraic form of the Eq.(27) indicates that the coupling of the probability p_n of an event and the "approximate" probability $1 - p_n$ of a "quasi" antievent is a necessary condition for the emergence of the sigmoid Weibullzian dynamics.

Note that, this coupling of probabilities is much more complex than that observed in the case of the iterative normalized Gompertz function. Analogously to the iterative normalized Gompertz model, the iterative normalized Weibull equation generates Feigenbaum-like diagrams, see Fig.2(a). Also in this case, as in the Gompertz model, to be observable a chaotic behavior is necessary to consider high values of r, see numerical results of Table 1. The Weibull equation (27) reflects the equilibrium between regular and chaotic states in the system with Weibullzian dynamics.

In a similar way, from the Eq.(25), and using Euler's algorithm, results the iterative normalized Fréchet equation

$$p_{n+1} = r\ p_n\left(\frac{1}{r} + (-\ln p_n)^{1+\frac{1}{\alpha}}\right) \tag{28}$$

with $r = a\ \alpha\ \Delta_t$, $\Delta_t \to 0$, $p_n = \frac{f_N(t_n)}{f_N(t_0)}$ and $\frac{1}{\alpha} > 0$. This difference equation describes the Frechetzian dynamics and represents also a complex non-linear coupling of probabilities. The "quasi" antagonistic events involved in this process have probabilities p_n and $1 - p_n$ "approximately". From the viewpoint of the non-linear coupling of probabilities, the models of the Fréchet type naturally exhibit chaotic behavior, for small values of the parameter r, according to the Eq.(28), see Fig.2(c) and numerical results of Table 1.

Subsequently, the complex dynamical behavior of the Weibullzian and Frechetzian dynamics is investigated.

5. **Dynamical approach.** The dynamical behavior study of the Weibull and Fréchet models is made using the dynamical systems theory, namely the symbolic dynamics and the iteration theory of unimodal maps. This study is completely characterized by the symbolic sequences associated to the critical point itinerary, see appendix for details. A remarkable contribution lies in the fact that the critical point be coincident with the number of cells when the growth rate is maximum.

In the sequence of the probability density function (3) and the differential equation (9), new dynamical systems are established. Considering the parameters values $p = 2$ and $q > 1$, these dynamical systems describe growths governed by Weibull ($1 < q < 2$), Gompertz ($q = 2$) and Fréchet ($q > 2$) distributions.

Thus, the family of maps proportional to the $Beta^*(2, q)$ densities are defined by $g_{\lambda,q} :]0, 1] \to [0, 1]$, such that

$$g_{\lambda,q}(x) = \lambda\ x\ \ (-\ln x)^{q-1} \tag{29}$$

where $x = f_N(t)$ is the normalized number of tumour cells or tumour size, $\lambda > 0$ is an intrinsic growth rate of the number of cells (individual contribution), that summarizes mutual inhibitions between cells and the competition for nutrients, and it is sometimes viewed as a retardation factor, and $q > 1$ is a shape parameter, that is sometimes called the growth-retardation factor. We request claim particular attention to the diversity and complexity of this family of models, which is exemplified in Fig.3. For each type of model, the several intrinsic growth rates were chosen in order to illustrate the growth rates of the various regions studied in this section.

The maps (29) is a family of unimodal maps, satisfying the following conditions:

- $g_{\lambda,q}(0^+) = g_{\lambda,q}(1) = 0$;
- $g_{\lambda,q} \in C^3\,(]\,0, 1\,[)$;
- $g'_{\lambda,q}(x) \neq 0, \forall x \in]0, 1[\backslash\{c\}$, with $c = N_{inf} = e^{1-q}$ the critical point of $g_{\lambda,q}$;
- $g'_{\lambda,q}(c) = 0$ and $g''_{\lambda,q}(c) < 0$;
- the Schwarz derivative of $g_{\lambda,q}(x)$ is given by

$$\begin{aligned} S\left(g_{\lambda,q}(x)\right) &= \frac{g'''_{\lambda,q}(x)}{g'_{\lambda,q}(x)} - \frac{3}{2}\left(\frac{g''_{\lambda,q}(x)}{g'_{\lambda,q}(x)}\right)^2 \\ &= -\frac{(q-1)\left(q\left(q^2-3q+2\right)+4q(q-2)\ln(x)-5(q-1)\ln^2(x)-2\ln^3(x)\right)}{2x^2\ln^2(x)\left(q-1+\ln(x)\right)^2}. \end{aligned}$$

It can be seen that $S\left(g_{\lambda,q}(x)\right) < 0$, for $x \in]0, 1[\backslash\{c\}$. This condition ensures a "good" dynamic behavior of the models: continuity and monotonicity of topological entropy, order in the succession of bifurcations, the existence of an upper limit to the number of stable orbits and the non-existence of wandering intervals, [15] and [26]. For some values at the beginning or at the end of the interval $]0, 1[$, it is verified

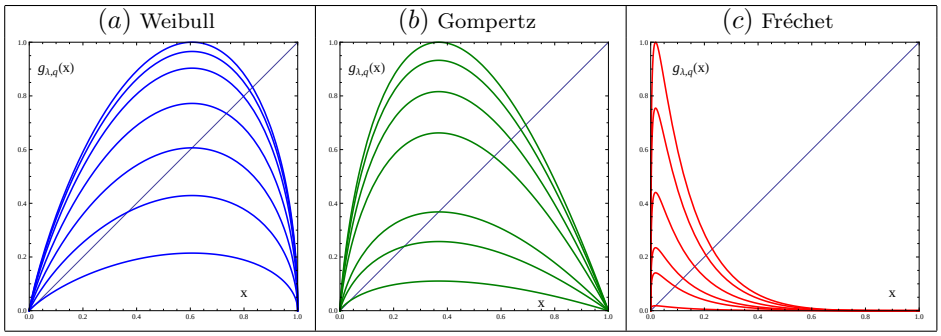

FIGURE 3. Growth rates of the number of tumour cells or tumour size defined by $g_{\lambda,q}$: Weibull for $q = 1.5$ and several intrinsic growth rates $\lambda = 0.5, 1, 1.4, 1.8, 2.1, 2.25, 2.33$; Gompertz for $q = 2$ and $\lambda = 0.3, 0.7, 1.0, 1.8, 2.22, 2.54, 2.72$; Fréchet for $q = 5$ and $\lambda = 0.004, 0.03, 0.05, 0.094, 0.161, 0.213$. The several intrinsic growth rates were chosen in order to illustrate growth rates of the various regions studied in the Subsec.5.1, see also Fig.4

that $S\left(g_{\lambda,q}(x)\right) \geq 0$. This failure in the conditions required for $g_{\lambda,q}$ be a unimodal map does not disturb the dynamical behavior. Note that, $S\left(g_{\lambda,q}(c)\right) = -\infty$ and the points $x = 0$ and $x = 1$ are repulsive.

5.1. **Regression, stability, bifurcation, chaos and terminus.** This subsection is devoted to the study of the complex dynamical behavior of the Weibull and Fréchet models. The complexity of these models, described by the maps $g_{\lambda,q}$, defined in (29), is displayed as a function of the parameters λ and q. Or, equivalently, the dynamical behavior is analyzed according to the intrinsic growth rate of the number of cells and the shape parameter q related with the growth-retardation phenomena. This complexity is measured in terms of topological entropy, see appendix for details. The parameter space is split into different regions, according to the chaotic behavior of the models, and reflects the natural history of the malignant tumour, see Fig.4. Similar studies were presented for the population growth logistic model and some types of coupling, see for example [11] and [12]. The dynamics of human hosts and tumours using bifurcation techniques and studying local stability can be seen, for example, in [6].

5.1.1. *Regression or spontaneous extinction region.* The spontaneous extinction or tumour regression region is characterized by growths models of very small tumours, possibly unable to outwit immune surveillance. In this region, the iterates of the maps $g_{\lambda,q}$ are always attracted to a fixed point x_0 sufficiently close to zero, with $q > 1$ and

$$0 < \lambda < \lambda_1(q) = \left(-\ln\left(x_0\right)\right)^{1-q}. \tag{30}$$

In this context, the concept of the fixed point x_0 "sufficiently close to zero" must be related to the specificity of the tumours growths investigation and clinical therapy. Thus, the spontaneous extinction region illustrated in Fig.4 is upper bounded by the curve $\lambda_1(q)$, considering $x_0 = 10^{-7}$. The symbolic sequences associated to the critical point orbits of these maps are of the type CL^{∞}, an aperiodic orbit, and its topological entropy is null, [10] and [16], see appendix.

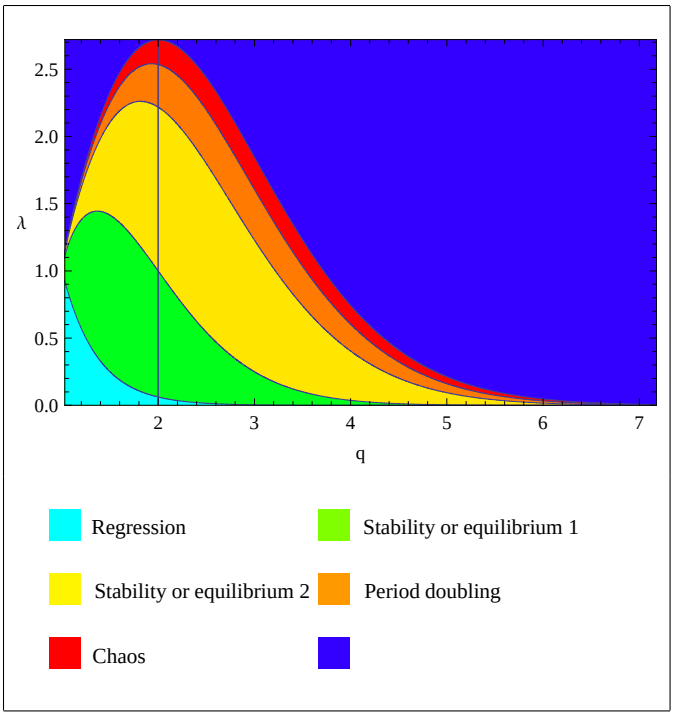

FIGURE 4. Bifurcation diagram for Eq.(29): plot of intrinsic growth rate λ versus growth-retardation phenomena q. The parameter space (q, λ) is splited into different regions, according to the dynamical behavior of the models: regression, stability or equilibrium, period doubling, chaos and terminus. The vertical line $q = 2$ correspond to the Gompertz model. The curves $\lambda_i(q)$, with $i = 1, 2, 3, 4, 5$, are represented in ascending order.

Remark. In the Fréchet model ($q > 2$), if $N_{inf} < N_0$ then $N_{inf} = e^{1-q} \to 0$, when $q \to +\infty$. On the other hand, the expression of the fixed points of $g_{\lambda,q}$, given by Eq.(30), goes to zero, when $\lambda \to 0^+$ and $q \to +\infty$, with a convergence rate higher than $N_{inf} = e^{1-q} \to 0$. This means that, to sufficiently small values of the intrinsic growth rate, the fixed point of $g_{\lambda,q}$ is below the critical point of the map. Since, $g_{\lambda,q}$ is a unimodal map then the symbolic sequences, corresponding to the orbit of the critical point, are CL^∞. The orbit of the critical point tends to the single fixed point, which goes to zero. So, we are dealing with a spontaneous extinction. Hence, the iterates of the growth of tumour cells, when the growth rate is maximum, goes to zero.

5.1.2. *Stability or equilibrium region.* In this region, the tumour growth remains stable and balanced without verifying growth duplications. Globally, the iterates of any map $g_{\lambda,q}$, whose parameters values belong to this region, are always attracted to the fixed point given by $(-\ln x)^{q-1} = \lambda^{-1}$, with $\lambda > 0$. This means that, the number of tumour cells or the tumour size remains fixed. This region is divided by a super stable or super attractive curve, defined by

$$\lambda_2(q) = (q-1)^{1-q}$$

with $q > 1$. For $\lambda_1(q) < \lambda < \lambda_2(q)$, the symbolic sequences associated to the critical point orbits are of the type CL^∞, an aperiodic orbit. On the other hand, for $\lambda_2(q) < \lambda < \lambda_3(q)$, the symbolic sequences associated to the critical point orbits are of the type CR^∞, an aperiodic orbit. The curve $\lambda_3(q)$, where the period doubling starts, is implicitly given by the equation

$$\lambda^2 \left(-\ln \left(\lambda e^{1-q} (q-1)^{q-1} \right) \right)^{q-1} = (q-1)^{1-q}.$$

The curve $\lambda_3(q)$, illustrated in Fig.4, is obtained using the values of intrinsic growth rate λ corresponding to the 2-period symbolic sequences $(CR)^\infty$. The unimodal maps $g_{\lambda,q}$ of this region do not exhibit chaotic behavior, its topological entropy being null, [10] and [16].

5.1.3. *Period doubling region.* The period doubling region corresponds to the parameters values to which the number of tumour cells or the tumour size will evolve between two values. A cascade of sudden changes provokes the oscillation of the (two possible) numbers of tumour cells or the tumour size in several limit cycles of period 2^n, with $n \in \mathbb{N}$. This period-doubling cascade is bounded by $\lambda_3(q) < \lambda < \lambda_4(q)$. The geometric representation of the curve $\lambda_4(q)$, in Fig.4, is determinated using values of intrinsic growth rate λ, corresponding to the first symbolic sequence with non null topological entropy. In the numerical results presented in Table 1, this symbolic sequence is $\left(CRLR^3\right)^\infty$, a 6-periodic orbit, that usually identifies the beginning of chaos. The unimodal maps $g_{\lambda,q}$ of this region also have null entropy, [10] and [16].

5.1.4. *Chaotic region.* In this region, the evolution of the number of tumor cells or tumor size is *a priori* unpredictable. This number may increase or decrease, it will depend on where the chaotic attractor in the phase space is located. The intrinsic growth rate of the cells number satisfies

$$\lambda_4(q) < \lambda < \lambda_5(q) = N_{inf}^{-1} (q-1)^{1-q}$$

where $N_{inf} = c = e^{1-q}$ is the number of cells when the growth rate is maximum. The iterates of the maps $g_{\lambda,q}$ originate orbits of several types, which already present chaotic patterns of behavior; so, its topological entropy is positive and the Sharkovsky order is verified. The value of the topological entropy increases with the value of the parameter λ, until reaches the maximum value ln 2 (consequence of the negative Schwartzian derivative), see Table 1, [15] and [16]. The full shift curve $\lambda_5(q)$, which is a maximum isentropic curve, is the graphic of a monotone function with an absolute maximum point in $q = 2$, corresponding to the Gompertz model.

5.1.5. *Terminal region.* The terminal phase describe the dynamics of the tumour growth while the host has survival conditions, until the host itself perishes from the tumour burden. In this region, where the intrinsic growth rate $\lambda > \lambda_5(p)$, the tumour growth rate stabilizes. At this stage, the dynamics leads to Cantor sets.

5.2. **Numerical results and discussion.** In Table 1 are showed the numerical results that illustrate the application of the iteration theory and the symbolic dynamics to Weibull, Gompertz and Fréchet models. It established a topological order, depending on the growth-retardation factor and on the intrinsic growth rate, which reflects the several phases of the tumour growth. Analyzing the results, it was concluded that:

Table 1: Topological order: intrinsic growth rate (λ) and topological entropy ($h_{top}\,(g_{\lambda,q})$) for growth-retardation factor q versus symbolic sequences $S^{(\lambda)}$ of period k.

k	$S^{(\lambda)}$	$q=1.3$	$q=1.5$	$q=1.8$	$q=2$	$q=2.5$	$q=3.5$	$q=5$	h_{top}
2	$(CR)^{\infty}$	1.8225	2.1063	2.2613	2.2184	1.7986	0.7417	0.0946	0.000
4	$(CRLR)^{\infty}$	1.8740	2.2064	2.4357	2.4343	2.0674	0.9355	0.1371	0.000
8	$(CRLR^3LR)^{\infty}$	1.8841	2.2264	2.4710	2.4784	2.1239	0.9786	0.1474	0.000
6	$(CRLR^3)^{\infty}$	1.8971	2.2519	2.5165	2.5357	2.1979	1.0360	0.1614	0.241
8	$(CRLR^5)^{\infty}$	1.9034	2.2646	2.5391	2.5642	2.2351	1.0654	0.1688	0.304
7	$(CRLR^4)^{\infty}$	1.9113	2.2802	2.5673	2.5997	2.2817	1.1027	0.1784	0.382
5	$(CRLR^2)^{\infty}$	1.9168	2.2911	2.5870	2.6247	2.3146	1.1294	0.1853	0.414
7	$(CRLR^2LR)^{\infty}$	1.9212	2.3000	2.6030	2.6450	2.3416	1.1514	0.1912	0.442
8	$(CRLR^2LR^2)^{\infty}$	1.9246	2.3067	2.6152	2.6605	2.3622	1.1683	0.1957	0.468
3	$(CRL)^{\infty}$	1.9273	2.3121	2.6250	2.6730	2.3789	1.1821	0.1994	0.481
6	$(CRL^2RL)^{\infty}$	1.9280	2.3136	2.6276	2.6763	2.3833	1.1858	0.2004	0.481
8	$(CRL^2RLR^2)^{\infty}$	1.9301	2.3177	2.6352	2.6860	2.3963	1.1966	0.2033	0.499
7	$(CRL^2RLR)^{\infty}$	1.9318	2.3210	2.6412	2.6936	2.4064	1.2050	0.2056	0.522
8	$(CRL^2RLRL)^{\infty}$	1.9329	2.3234	2.6454	2.6991	2.4137	1.2111	0.2073	0.539
5	$(CRL^2R)^{\infty}$	1.9333	2.3241	2.6467	2.7007	2.4159	1.2130	0.2078	0.544
8	$(CRL^2R^3L)^{\infty}$	1.9336	2.3248	2.6480	2.7023	2.4181	1.2141	0.2083	0.547
7	$(CRL^2R^3)^{\infty}$	1.9345	2.3265	2.6511	2.7063	2.4234	1.2192	0.2095	0.562
8	$(CRL^2R^4)^{\infty}$	1.9352	2.3280	2.6538	2.7098	2.4281	1.2232	0.2106	0.574
6	$(CRL^2R^2)^{\infty}$	1.9357	2.3288	2.6553	2.7117	2.4307	1.2253	0.2112	0.584
8	$(CRL^2R^2LR)^{\infty}$	1.9360	2.3294	2.6565	2.7132	2.4327	1.2270	0.2117	0.591
7	$(CRL^2R^2L)^{\infty}$	1.9363	2.3300	2.6576	2.7146	2.4346	1.2287	0.2121	0.601
4	$(CRL^2)^{\infty}$	1.9365	2.3304	2.6584	2.7155	2.4359	1.2297	0.2124	0.609
∞	CRL^{∞}	1.9371	2.3316	2.6605	2.7183	2.4395	1.2328	0.2133	$\ln 2$

- Monotonicity of the topological entropy: if the number of cells when the growth rate is maximum is fixed and the intrinsic growth rate increases, then the topological entropy is a non-decreasing function in order to the parameter λ. Thus, the intrinsic growth rate determines the convergence rate to the normalized carrying capacity (observed in the last column of Table 1).
- Isentropic curves: if the number of cells when the growth rate is maximum varies then, for each of these values, there is an intrinsic growth rate λ such that the topological entropy is constant (observed in each row of Table 1).
- If the number of cells when the growth rate is maximal decreases, in each isentropic curve, then the intrinsic growth rate is a monotonic function with an absolute maximum point, corresponding to the Gompertz model (observed in each row of Table 1).

We believe that more results can be derived from the study of the dynamical systems that describe these models. In particular, the analysis of the bifurcations structure, based on the configurations of fold and flip bifurcation curves, and the study of the respective basins.

Acknowledgments. This research has been supported by National Funds through FCT - Fundação para a Ciência e a Tecnologia, project PEst-OE/MAT/UI0006/2011, and PTDC/FEDER. The authors thank the editor and the referees for their careful reading and helpful comments, which lead to a huge improvement on the presentation of the original manuscript. The authors are also grateful to Prof. Danièle Fournier-Prunaret for constructive discussions and remarks on the work. Finally, we thank Prof. Júlia Teles by her careful reading of the paper.

Appendix: Symbolic dynamics and topological entropy. Symbolic dynamics is a theory composed by a set of results, methods and techniques, which have a primordial role in the study of qualitative and quantitative properties of discrete dynamical systems. The topological complexity of a dynamical system is usually measured by its topological entropy. This numerical and topological invariant is associated to the growth rate of the several states of dynamical systems, [10], [15], [16] and [22].

Consider for each value of the parameter λ, the orbit of the critical point $c = N_{inf}$

$$O_\lambda(c) = \left\{x_k : x_k = g^k_{\lambda,q}(c),\ k \in \mathbb{N}_0\right\}$$

defined by an iterative process, where $x_k = g^k_{\lambda,q}(c) = g_{\lambda,q}(x_{k-1})$. Thus, for each value of the intrinsic growth rate is considered the orbit of the number of cells when the growth rate is maximum. In order to study the topological properties of these orbits, we associate to each orbit $O_\lambda(c)$ a sequence of symbols, corresponding to the critical point itinerary, denoted by $S^{(\lambda)} = S^{(\lambda)}_0 S^{(\lambda)}_1 S^{(\lambda)}_2 \ldots S^{(\lambda)}_k \ldots$, with $k \in \mathbb{N}_0$, where $S^{(\lambda)}_k$ belongs to the alphabet $\mathcal{A} = \{L, C, R\}$, with each symbol defined by

$$S^{(\lambda)}_k = \begin{cases} L & \text{if } g^k_{\lambda,q}(c) < c \\ C & \text{if } g^k_{\lambda,q}(c) = c \\ R & \text{if } g^k_{\lambda,q}(c) > c \end{cases}.$$

Note that, the alphabet $\mathcal{A}$ is an ordered set of symbols, corresponding to the intervals of monotonicity and to the critical point of the map $g_{\lambda,q}$. The real line order induces naturally an order relation in the alphabet $\mathcal{A}$, so $L \prec C \prec R$. The space of all symbolic sequences of the alphabet $\mathcal{A}$ is denoted by $\mathcal{A}^{\mathbb{N}}$.

The expansive maps admit Markov partitions, whose existence is implicit in the works of Bowen and Ruelle. In this study, we consider the existence of Markov partitions, which are characterized by the orbit of the critical point of the map $g_{\lambda,q}$, [22]. Consider the set of points corresponding to the k-periodic orbit or kneading sequence of the critical point $S^{(\lambda)} = (CS^{(\lambda)}_1 S^{(\lambda)}_2 \ldots S^{(\lambda)}_{k-1})^\infty \in \mathcal{A}^{\mathbb{N}}$. This set of points determines the Markov partition of the interval $I = \left[g^2_{\lambda,q}(c), g_{\lambda,q}(c)\right]$ in a finite number of subintervals, denoted by $\mathcal{P}_I = \{I_1, I_2, \ldots, I_{k-1}\}$. The dynamics of the map $g_{\lambda,q}$ is completely characterized by the symbolic sequence $S^{(\lambda)}$ associated to the critical point itinerary. The map $g_{\lambda,q}$ and the Markov partition associated induce a subshift of finite type whose Markov transition matrix $A = [a_{ij}], (k-1) \times (k-1)$, is defined by

$$a_{ij} = \begin{cases} 1, & \text{if } int\,(I_j) \subseteq g_{\lambda,q}(int\,(I_i)) \\ 0, & \text{otherwise} \end{cases}.$$

Usually, the subshift is denoted by $(\sum_A, \sigma)$, where σ is a shift map in $\sum^{\mathbb{N}}_{k-1}$ defined by $\sigma\,(S_1 S_2 \ldots) = S_2 S_3 \ldots$, with $\sum_{k-1} = \{1, \ldots, k-1\}$ corresponding to the $k-1$ subshifts states.

The topological entropy of the map $g_{\lambda,q}$, in the phases space, is defined in the associated symbolic space as the asymptotic growth rate of the admissible words (finite symbolic sequences) in relation to the length of the words, i.e.,

$$h_{top}\,(g_{\lambda,q}) = \lim_{n\to\infty} \frac{\ln N\,(n)}{n}$$

where $N\,(n)$ is the number of admissible words of length n. For a subshift of finite type, unidirectional or bidirectional, described by the Markov transition matrix A, the topological entropy is given by $h_{top}\,(\sigma) = \ln\,(\lambda_A)$, where λ_A is the spectral

radius of the transition matrix A. For a more detailed approach about subshifts of finite type and the Perron-Frobenius Theorem for Markov transition matrix, see [10], [15], [22] and references therein.

REFERENCES

[1] S. M. Aleixo, J. L. Rocha and D. D. Pestana, *Populational growth models proportional to beta densities with Allee effect*, AIP Conf. Proc. American Inst. of Physics, **1124** (2009), 3–12.

[2] S. M. Aleixo, J. L. Rocha and D. D. Pestana, *Dynamical behavior on the parameter space: new populational growth models proportional to beta densities*, Proc. Int. Conf. on Information Technology Interfaces, (2009), 213–218.

[3] S. M. Aleixo, J. L. Rocha and D. D. Pestana, *Probabilistic methods in dynamical analysis: populations growths associated to models Beta(p, q) with Allee effect*, in "Dynamics, Games and Science II" (eds. M. M. Peixoto, A. A. Pinto and D. A. J. Rand), Springer-Verlag (2011), 79–95.

[4] A. A. Blumberg, *Logistic growth rate functions*, J. of Theoret. Biol., **21** (1968), 42–44.

[5] C. W. Clark, "Mathematical Bioeconomics: The Optimal Management of Renewable Resources," John Wiley & Sons, Inc., New York, 1990.

[6] D. Kirschner and A. Tsygvintsev, *On the global dynamics of a model for tumor immunotherapy*, Math. Biosci. Eng., **6** (2009), 573–583.

[7] F. Kozusko and Z. Bajzer, *Combining gompertzian growth and cell population dynamics*, Math. Biosci., **185** (2003), 153–167.

[8] A. K. Laird, *Dynamics of tumour growth*, Br. J. Cancer, **18** (1964), 490–502.

[9] A. K. Laird, S. A. Tyler and A. D. Barton, *Dynamics of normal growth*, Growth, **29** (1965), 233–248.

[10] D. Lind and B. Marcus, "An Introduction to Symbolic Dynamics and Codings," Cambridge University Press, Cambridge, 1995.

[11] R. López-Ruiz and D. Fournier-Prunaret, *Complex behavior in a discrete coupled logistic model for the symbiotic interaction of two species*, Math. Biosci. Eng., **1** (2004), 307–324.

[12] R. López-Ruiz and D. Fournier-Prunaret, *Periodic and chaotic events in a discrete model of logistic type for the competitive interaction of two species*, Chaos, Solitons & Fractals, **41** (2009), 334–347.

[13] A. S. Martinez, R. S. González and C. A. S. Terçariol, *Continuous growth models in terms of generalized logarithm and exponential functions*, Physica A, **387** (2008), 5679–5687.

[14] M. Marušić and Ž. Bajzer, *Generalized two-parameter equation of growth*, J. Math. Anal. Appl., **179** (1993), 446–462.

[15] W. Melo and S. van Strien, "One-Dimensional Dynamics," Springer, New York, 1993.

[16] J. Milnor and W. Thurston, *On iterated maps of the interval*, Dynamical systems (College Park, MD, 1986C87), 465–563, Lecture Notes in Math., 1342, Springer, Berlin, 1988.

[17] M. Molski and J. Konarsky, *On the Gompertzian growth in the fractal space-time*, BioSystems, **92** (2008), 245–248.

[18] A. d'Onofrio, *A general framework for modeling tumor-imune system competition and immunotherapy: Matematical analysis and biomedical inferences*, Physica D, **208** (2005), 220–235.

[19] A. d'Onofrio, A. Fasano and B. Monechi, *A generalization of Gompertz law compatible with the Gyllenberg-Webb theory for tumour growth*, Math. Biosciences, **230** (2011), 45–54.

[20] D. D. Pestana and S.Velosa, "Introdução à Probabilidade e à Estatística," Fundação Calouste Gulbenkian, Lisboa, 2008.

[21] D. D. Pestana, S. M. Aleixo and J. L. Rocha, *Regular variation, paretian distributions, and the interplay of light and heavy tails in the fractality of asymptotic models*, in "Chaos Theory: Modeling, Simulation and Applications" (eds. C. H. Skiadas, Y. Dimotikalis and C. Skiadas), World Scientific Publishing Co, (2011), 309–316.

[22] J. L. Rocha and J. Sousa Ramos, *Weighted kneading theory of one-dimensional maps with a hole*, Int. J. Math. Math. Sci., **38** (2004), 2019–2038.

[23] J. L. Rocha and S. M. Aleixo, *Dynamical analysis in growth models: Blumberg's equation*, Discrete Contin. Dyn. Syst.-Ser.B, **18** (2013), 783–795.

[24] S. Sakanoue, *Extended logistic model for growth of single-species populations*, Ecol. Model., **205** (2007), 159–168.

[25] H. Schättler, U. Ledzewicz and B. Cardwell, *Robustness of optimal controls for a class of mathematical models for tumor anti-angiogenesis*, Math. Biosci. Eng., **8** (2011), 355–369.
[26] D. Singer, *Stable orbits and bifurcations of maps of the interval*, SIAM J. Appl. Math., **35** (1978), 260–267.
[27] A. Tsoularis , *Analysis of logistic growth models*, Res. Lett. Inf. Math. Sci., **2** (2001), 23–46.
[28] M. E. Turner Jr., E. L. Bradley Jr., K. A. Kirk and K. M. Pruitt, *A theory of growth*, Math. Biosci., **29** (1976), 367–373.
[29] P. Waliszewski and J. Konarski, *The gompertzian curve reveals fractal properties of tumour growth*, Chaos Solitons & Fractals, **16** (2003), 665–674.
[30] P. Waliszewski and J. Konarski, *A mystery of the Gompertz function*, in "Fractals in Biology and Medicine" (eds. G. A. Losa, T. F. Nonnenmacher and E. R. Weibel), Birkhäuser, Basel, (2005), 277–286.
[31] P. Waliszewski, *A principle of fractal-stochastic dualism and Gompertzian dynamics of growth and self-organization*, Byosystems, **82** (2005), 61–73.
[32] P. Waliszewski, *A principle of fractal-stochastic dualism, couplings, complementarity growth*, J. Control Eng. and Appl. Informatics, **4** (2009), 45–52.

Received February 27, 2012; Accepted October 09, 2012.

E-mail address: jrocha@adm.isel.pt
E-mail address: sandra.aleixo@adm.isel.pt